CHEMISTRY OF MATERIALS
Article

Chem. Mater. **2009,** *21,* 4163–4171 4163
DOI:10.1021/cm900339h

New Monofunctional POSS and Its Utilization as Dewetting Additive in Methacrylate Based Free-Standing Films

Fayna Mammeri,*[,†,∥] Christian Bonhomme,[‡,§] François Ribot,[‡,§] Florence Babonneau,[‡,§] and Sandra Dirè[†]

[†]*Dipartimento di Ingegneria dei Materiali e Tecnologie Industriali, Università di Trento, Via Mesiano 77, 38050 Trento, Italy,* [‡]*UPMC Univ. Paris 06 and* [§]*CNRS, UMR 7574, Chimie de la Matière Condensée de Paris, Collège de France, 11 place Marcelin Berthelot, 75231 Paris Cedex 05, France.* [∥]*Permanent address: Laboratoire Interfaces, Traitements, Organisation et Dynamique des Systèmes (ITODYS), Université Paris-Diderot Paris 7, UMR CNRS 7086, Bâtiment Lavoisier, 15 rue Jean de Baïf, 75205 Paris Cedex 13, France.*

Received February 5, 2009. Revised Manuscript Received July 27, 2009

New polyhedral oligomeric silsesquioxanes (POSS), (^{i}BuSi)$_7$O$_{12}$SiOSi(Me)$_2$CH$_2$(CH$_2$)$_n$CH$_2$OC(O)C(CH$_3$)=CH$_2$ bearing one *single* methacrylate group, were synthesized by hydrosilylation of allylalcohol or 4-penten-1-ol, followed by acylation with methacryloyl chloride. All intermediates and final derivatives were carefully characterized by FTIR, ^{1}H, ^{13}C, and ^{29}Si solution state NMR, size exclusion chromatography (SEC), MALDI-TOF MS, and powder XRD (including full indexation of the diffraction patterns). In a second step, POSS/methacrylate based films were prepared. For 10 wt % of POSS, phase separation occurs with concomitant POSS crystallization. This behavior is not observed for 2 wt %, but XPS analyses show migration of POSS toward the film−air interface, which led to improved hydrophobic properties of the UV polymerized films with a 30° increase in contact angle.

Introduction

It is now well-established that organic/inorganic hybrid materials offer new scientific opportunities in the frame of multifunctional nanomaterials.[1] An elegant approach to achieving well-defined nanocomposites consists of the use of preformed inorganic objects (nano building blocks or NBBs) such as metal-oxo-clusters (Si, Ti, Zr, Sn, etc.), nanoparticles, or nanolayered compounds[2,3] bearing functionalities that allows for their anchoring to the organic matrix. The objective is generally to reach in the final composite homogeneous distribution of nanometric and perfectly defined nano-objects. We focused here on cubane shaped silsesquioxanes (polyhedral oligomeric silsesquioxanes or POSS),[4] mostly studied for various applications,[5] in the fields of dental materials,[6] catalysts,[7] flame retardants,[8] low-*k* dielectric materials,[9] resist coatings for lithography,[10] or high-temperature lubricants.[11] Their properties can be adjusted by appropriate introduction of organic functions that are covalently bonded to the Si_8O_{12} core either through a Si−C bond or a short Si−O−Si spacer, often a dimethylsiloxy group.

Among functionalized POSS, two main families can be distinguished. Polyfunctional POSS can be used as cross-linkers for polymers or as a main component in the

*To whom all correspondence should be addressed. E-mail: fayna.mammeri@univ-paris-diderot.fr.

(1) (a) Eckert, H., Ward, M., Eds. Special Issue: Organic−Inorganic Nanocomposite Materials. Chem. Mater. **2001**, *13* (10). (b) Sanchez, C., Ed. Special Issue on Functional Hybrid Materials. J. Mater. Chem. **2005**, *15* (35−36). (c) Sanchez, C.; Boissiere, C.; Grosso, D.; Laberty, C.; Nicole, N. *Chem. Mater.* **2008**, *20*, 682–737.
(2) (a) Ribot, F.; Sanchez, C. *Comments Inorg. Chem.* **1999**, *20*, 327–371. (b) Sanchez, C.; Soler-Illia, G. J. A. A.; Ribot, F.; Lalot, T.; Mayer, C. R.; Cabuil, V. *Chem. Mater.* **2001**, *13*, 3061–3083.
(3) Kickelbick, G. *Prog. Polym. Sci.* **2003**, *28*, 83–114.
(4) (a) Voronkov, M. G.; Lavrent'yev, V. I. *Top. Curr. Chem.* **1982**, *102*, 199–236. (b) Lichtenhan, J. D. *Comments Inorg. Chem.* **1995**, *17*, 115–130. (c) Provatas, A.; Matisons, J. G. *Trends Polym. Sci.* **1997**, *5*, 327–332. (d) Phillips, S. H.; Haddad, T. S.; Tomczak, S. J. *Curr. Opin. Solid State Mater. Sci.* **2004**, *8*, 21–29. (e) Chojnowski, J.; Fortuniak, W.; Rosciszewski, P.; Werel, W.; Lukasiak, J.; Kamysz, W.; Halasa, R. *J. Inorg. Organomet. Polym. Mater.* **2006**, *16*, 219–230. (f) Peng, Y.; McCabe, C. *Mol. Phys.* **2007**, *105*, 261–272. (g) Liu, L.; Tian, M.; Zhang, W.; Zhang, L. Q.; Mark, J. E. *Polymer* **2007**, *48*, 3201–3212. (h) Takamura, N.; Viculis, L.; Zhang, C.; Laine, R. M. *Polym. Int.* **2007**, *56*, 1378–1391. (i) Laine, R. M.; Roll, M.; Asuncion, M.; Sulaiman, S.; Popova, V.; Bartz, D.; Krug, D. J.; Mutin, P. H. *J. Sol Gel Sci. Technol.* **2008**, *46*, 335–347. (j) Lickiss, P. D.; Rataboul, F. *Adv. Organomet. Chem.* **2008**, *57*, 1–116. (k) Zhang, W. A.; Liu, L.; Zhuang, X. D.; Li, X. H.; Bai, J. R.; Chen, Y. *J. Polym. Sci., Part A* **2008**, *46*, 7049–7061. (l) Boury, B. *Silicon Based Polymers: Advances in Synthesis and Supramolecular Organization* **2008**, 233–246.
(5) Pielichowski, K.; Njuguna, J.; Janowski, B.; Pielichowski, J. In *Supramolecular Polymers Polymeric Betains Oligomers*; Springer-Verlag Berlin: Berlin, 2006; Vol. *201*, pp 225−296.
(6) Fong, H.; Dickens, S. H.; Flaim, G. M. *Dental Mater.* **2005**, *21*, 520–529.
(7) Feher, F. J.; Budzichowski, T. A. *Polyhedron* **1995**, *14*, 3239–3253.
(8) Gupta, S. K.; Schwab, J. J.; Lee, A.; Fu, B. X.; Hsiao, B. S. *Int. SAMPE Symp. Exhib.* **2002**, *47*, 1517–1526.
(9) Su, R. Q.; Muller, T. E.; Prochazka, J.; Lercher, J. A. *Adv. Mater.* **2002**, *14*, 1369–1373.
(10) Bellas, V.; Tegou, E.; Raptis, I.; Gogolides, E.; Argitis, P.; Iatrou, H.; Hadjichristidis, N.; Sarantopoulo, E.; Cefalas, A. C. *J. Vac. Sci. Technol., B* **2002**, *20*, 2902–2908.
(11) Blanski, R.; Leland, J.; Viers, B.; Phillips, S. H. *Int. SAMPE Symp. Exhib.* **2002**, *47*, 1503–1507.

Published on Web 08/27/2009

elaboration of hybrid materials.[12,13] As so, they can be considered as network former in the classical glass terminology. Recently, Laine et al. described state-of-art syntheses and functionalization of octafunctional POSS as precursors for hybrid organic−inorganic materials.[14] In comparison, monofunctional POSS with only one reactive organic group can behave as dangling objects along polymeric backbones and thus act as network modifier.[15] In that case, they are expected to alter the properties of the polymer matrix. Thermomechanical properties of polymethylmethacrylate/POSS systems have been evaluated,[16,17] and tendency for monofunctional POSS toward aggregation was evidenced. This feature, which can be seen as negative if one looks for homogeneous distribution of nano-objects acting as nanocharges, can also be exploited to induce gradients of composition, thus causing enrichment in hydrophobic POSS at specific interfaces and modification of surface properties. This was already exploited to develop POSS-based methacrylate resists[18] with improved resistance against reactive ion etching in O_2 plasma.[19] Enrichment of the surface in POSS can also affect the surface wetting properties. Dispersion of POSS into polystyrene thin films deposited on Si wafers strongly influenced their dewetting behavior.[20,21] Along the same line, Esker et al.[22] also described the interesting behavior of telechelic poly(ethylene glycol)−POSS amphiphiles at the air/water interface.

The objective of this work was to prepare by photopolymerization polymethacrylate-based films containing various amounts of novel monofunctional methacryloxyalkyl-POSS and to characterize how the dispersion of the POSS entities into the films influences their surface properties, especially in terms of wetting. Our choice was to design POSS with a methacrylate group hanging at the end of a relatively mobile spacer compared to the commercially available $R_7Si_8O_{12}$ (propylmethacrylate). We thus performed the anchoring of propyl and pentyl methacrylate groups via a Si−O−Si linkage, starting from the commercial dimethylsiloxy isobutyl POSS (DMIPOSS), $(^{i}BuSi)_7O_{12}SiOSiMe_2H$. A similar polyfunctional POSS, the octamethacrylateoctasilsesquioxane has been synthesized by a direct regioselective hydrosilylation of allylalcohol with octakis(dimethylsiloxy)octasilsesquioxane ($Q_8M_8^H$), followed by acylation with methacryloylchloride.[23] Hydrosilylation of unsaturated OH terminated short poly(ethylene glycol) was also reported for the complete functionalization of $Q_8M_8^H$.[24] However, to the best of our knowledge monofunctional POSS bearing one propylmethacrylate group attached through a Si−O−Si link has been only partially described so far in the literature.[25,26] The present paper reports thus the synthesis of novel hydroxyalkyl and methacrylate functionalized cubane clusters from DMIPOSS. Hydrosilylation between two unsaturated alcohols with different chain length and DMIPOSS was first performed to produce new hydroxyalkyl-DMIPOSS, which were then reacted with methacryloyl chloride to obtain new methacryloxyalkyl-DMIPOSS derivatives. All intermediate and final derivatives were systematically characterized by various techniques including ^{1}H, ^{13}C, and ^{29}Si solution state NMR. The new compounds are all crystalline, and their powder XRD patterns were indexed with hexagonal cells. These results led to a discussion on the description of POSS packing in relation with a simple cubic network, a proposition that agrees better with the results observed than the generally considered hexagonal close packing of spheres on a fcc network.

Thus, polymethacrylate-based free-standing films derived from our novel precursors were prepared by photopolymerization, from a mixture of methacrylate resin monomers and various amounts of POSS (1, 2, and 10 wt %) deposited on a glass plate. XPS, SEM, and contact angle measurements led to sharp relationships between chemical composition and wetting properties of both film surfaces, initially in contact with air or glass plate. Very interestingly, a dissymmetric enrichment in POSS was observed in the free-standing films: POSS were found to preferentially pack at the surface in contact with air, leading to improved hydrophobic properties of the methacrylate resin. This dissymmetry will be discussed in relation with the sample preparation method.

(12) Castelvetro, V.; Ciardelli, F.; De Vita, C.; Puppo, A. *Macromol. Rapid Commun.* **2006**, *27*, 619–625.
(13) (a) Hoebbel, D.; Endres, K.; Reinert, T.; Pitsch, I. *J. Non-Cryst. Solids* **1994**, *176*, 179–188. (b) Laine, R. M.; Zhang, C.; Sellinger, A.; Viculis, L. *Appl. Organomet. Chem.* **1998**, *12*, 715–723. (c) Zhang, C. X.; Babonneau, F.; Bonhomme, C.; Laine, R. M.; Soles, C. L.; Hristov, H. A.; Yee, A. F. *J. Am. Chem. Soc.* **1998**, *120*, 8380–8391. (d) Laine, R. M.; Choi, J. W.; Lee, I. *Adv. Mater.* **2001**, *13*, 800–803. (e) Choi, J.; Harcup, J.; Yee, A. F.; Zhu, Q.; Laine, R. M. *J. Am. Chem. Soc.* **2001**, *123*, 11420–11430. (f) Choi, J.; Yee, A. F.; Laine, R. M. *Macromolecules* **2003**, *36*, 5666–5682. (g) Choi, J.; Kim, S. G.; Laine, R. M. *Macromolecules* **2004**, *37*, 99–109. (h) Markovic, E.; Clarke, S.; Matisons, J.; Simon, G. P. *Macromolecules* **2008**, *41*, 1685–1692.
(14) (a) Laine, R. M. *J. Mater. Chem.* **2005**, *15*, 3725–3744. (b) Roll, M. F.; Asuncion, M. Z.; Kampf, J.; Laine, R. M. *ACS Nano* **2008**, *2*, 320–326.
(15) (a) Lichtenhan, J. D.; Otonari, Y. A.; Carr, M. J. *Macromolecules* **1995**, *28*, 8435–8437. (b) Lichtenhan, J. D.; Noel, C. J.; Bolf, A. G.; Ruth, P. N. *Mater. Res. Soc. Symp. Proc.* **1996**, *435*, 3–11. (c) Schwab, J. J.; Lichtenhan, J. D. *Appl. Organomet. Chem.* **1998**, *12*, 707–713. (d) Turri, S.; Levi, M. *Macromolecules* **2005**, *38*, 5569–5574. (e) Zhang, S. L.; Zou, Q. C.; Wu, L. M. *Macromol. Mater. Eng.* **2006**, *291*, 895–901. (f) Zucchi, I. A.; Galante, M. J.; Williams, R. J. J.; Franchini, E.; Galy, J.; Gerard, J. F. *Macromolecules* **2007**, *40*, 1274–1282. (g) Wu, J.; Haddad, T. S.; Kim, G. M.; Mather, P. T. *Macromolecules* **2007**, *40*, 544–554.
(16) Kopeski, E. T.; Haddad, T. S.; Cohan, R. E.; McKinley, G. H. *Macromolecules* **2004**, *37*, 8992–9004.
(17) Bizet, S.; Galy, J.; Gérard, J.-F. *Macromolecules* **2006**, *39*, 2574–2583.
(18) Tegou, E.; Bellas, V.; Gogolides, E.; Argitis, P.; Eon, D.; Cartry, G.; Cardinaud, G. *Chem. Mater.* **2004**, *16*, 2567–2577.
(19) Koh, K.; Sugiyama, S.; Morinaga, T.; Ohno, K.; Tsujii, Y.; Fukuda, T.; Yamahiro, M.; Iijima, T.; Oikawa, H.; Watanabe, K.; Miyashita, T. *Macromolecules* **2005**, *38*, 1264–1270.
(20) Hosaka, N.; Otsuka, H.; Hino, M.; Takahara, A. *Langmuir* **2008**, *24*, 5766–5772.
(21) Paul, R.; Karabiyik, U.; Swift, M. C.; Hottle, J. R.; Esker, A. R. *Langmuir* **2008**, *24*, 4676–4684.
(22) Lee, W.; Ni, S.; Deng, J.; Kim, B. S.; Satija, S. K.; Mather, P. T.; Esker, A. R. *Macromolecules* **2007**, *40*, 682–688.
(23) Zhang, C.; Laine, R. M. *J. Am. Chem. Soc.* **2000**, *122*, 6979–6988.
(24) Markovic, E.; Ginic-Markovic, M.; Clarke, S.; Matisons, J.; Hussain, M.; Simon, G. P. *Macromolecules* **2007**, *40*, 2694–2701.
(25) Mammeri, F.; Douja, N.; Bonhomme, C.; Ribot, F.; Babonneau, F.; Dire, S. *Mater. Res. Soc. Symp. Proc.* **2005**, *847*, 363–368.
(26) Kiyomori, A.; Kubota, T.; Kubota, Y.; Honma, T. European Patent EP 1 645 560 A1, **2006**.

Scheme 1. Reactions of Allylalcohol or 4-Penten-1-ol and DMIPOSS: Competition between Hydrosilylation and Dehydrogenation

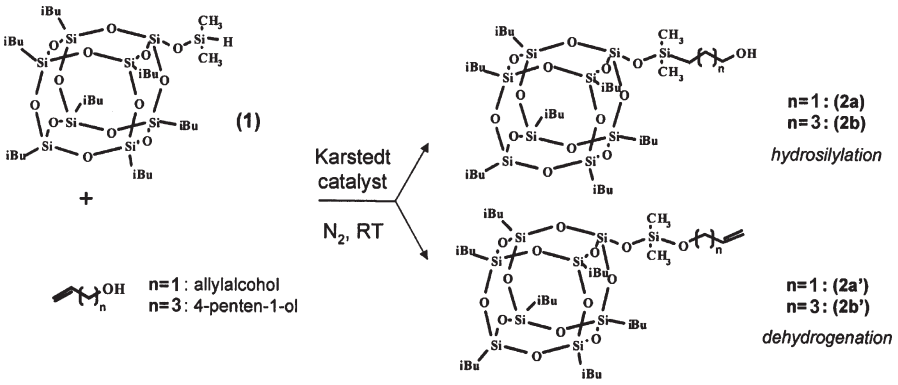

Experimental Section

Materials. *DMIPOSS Derived Compounds.* DMIPOSS, (^{i}BuSi)$_7$O$_{12}$SiOSiMe$_2$H (**1**), was purchased from Hybrid Plastics. Allylalcohol and methacryloylchloride were obtained from Fluka, 4-penten-1-ol and Karstedt's catalyst from ABCR-Gelest, triphenylphosphine and allylamine from Aldrich. Toluene was dried by distillation over Na/benzophenone before use; acetonitrile was dried over molecular sieves. The other products were used as received. For hybrid materials preparation, (^{i}Bu)$_7$Si$_8$O$_{12}$(propylmethacrylate) (^{i}BuPOSSMA, T_m = 109 °C) from Hybrid Plastics, cyclohexylmethacrylate (CHMA) from Aldrich, and tetra-ethoxylatedbisphenol A dimethacrylate (Bis-EMA) from Cray Valley Co. were used as received. The photocuring set was composed of Darocur 1173 and benzophenone, from Ciba-Geigy and *N*-methyl diethanol amine from Aldrich. The full characterization of DMIPOSS (**1**) (^{13}C, ^{1}H solution state NMR, MALDI-TOF, elemental analyses) is presented in the Supporting Information, as well as the syntheses of hydroxypropyl-DMIPOSS (**2a**), hydroxypentyl-DMIPOSS (**2b**), methacryloxypropyl-DMIPOSS (**3a**), and methacryloxypentyl-DMIPOSS (**3b**) (see also Schemes 1 and 2).[25] ^{1}H, ^{13}C NMR, MALTI-TOF and chemical analyses data for **2a**, **2b**, **3a**, and **3b** are also summarized in Supporting Information.

Hybrid Coatings and Free-Standing Films Preparation. Coatings were prepared by mixing 1, 2, or 10 wt % of monofunctional POSS (**3a**, **3b** and ^{i}BuPOSSMA) to a mixture of CHMA/Bis-EMA = 50/50 (w/w) (for each composition, a total of 2 g was prepared). Cyclohexylmethacrylate was used as a comonomer due to the weak POSS solubility into Bis-EMA.[17] The three monomers and the photocuring set (benzophenone, Darocur 1173, and methyldiethanolamine) were mixed at RT (2 wt % for each of the three compounds with respect to the monomer weight). Then, the homogeneous reactive mixtures were poured on hydrophilic float-glass plates with Teflon walls to prepare 100 μm thick films and spread homogeneously with the aid of a bar-coater. The thicknesses of the final films have been assessed ($\pm$0.5 μm) with a laser interferometer. Samples were then irradiated for ca. 70 s with an UV light lamp (Fusion F300, Fusion UV Systems Inc., power: 120 W·cm^{-1}). After polymerization, coatings were easily peeled-off from the glass plate to yield transparent free-standing films.

Structural Characterizations. The different reaction steps were monitored by ATR-FTIR on a Nicolet Magna IR 550 spectrometer (equipped with a ZnSe crystal, 45° incidence angle, 16 scans, 4 cm^{-1} resolution). At the end of the modification process, transmittance spectra were obtained on dry powders for products **3a** and **3b** dispersed in KBr pellets (64 scans, 4 cm^{-1} resolution).

^{29}Si and ^{13}C NMR experiments (including DEPT-135) were recorded on a Bruker AVANCE 400 spectrometer. ^{29}Si NMR spectra were recorded at 79.49 MHz, and chemical shifts were referenced to Si(CH$_3$)$_4$ (TMS). ^{29}Si sites were labeled with the conventional notation (M, D, T, Q). ^{13}C NMR spectra were collected at 100.62 MHz, and CDCl$_3$ was used as internal reference (77.3 ppm).[27] ^{1}H NMR experiments were performed in CDCl$_3$, using 5 mm tubes and recorded on a Bruker AC300 spectrometer (300.13 MHz). CHCl$_3$ impurity of CDCl$_3$ was used as internal reference (7.26 ppm).[27]

The thermogravimetric analyses (TGA) were performed under air or argon flow (100 mL·min^{-1}) on a Netzsch STA 414 equipment with a 10 °C·min^{-1} heating rate. Differential scanning calorimetry measurements were done under nitrogen atmosphere on a TA Instruments DSC 2010 thermal analyzer. Samples were equilibrated at 35 °C, heated to the desired temperature (between 150 and 275 °C depending on the sample) with a heating rate of 10 °C·min^{-1}, and allowed to cool down at 10 °C·min^{-1}.

The X-ray powder diffraction patterns were collected on a Rigaku DMax III diffractometer, using the Cu Kα radiation (λ = 1.5417 Å). The measurements were performed in Bragg–Brentano configuration. The scan range was 2–50° (2θ) with a step interval of 0.05° and a counting time of 5s. Powder XRD data were analyzed (6–50° in 2θ), with FullProf and WinPLOTR.[28,29]

Number-average molecular weights (M_n's), weight-average molecular weights (M_w's), and molecular weight-distributions (M_w/M_n's) were determined with size exclusion chromatography (SEC) using a series of Viscotek G2000 and G3000 columns (molecular weights lower than 40 000) and a RI detector (Viscotek VE3580). THF has been used as mobile phase with a flow rate of 1 mL·min^{-1}, and results were analyzed with the software OmniSec in conjunction with a PS standard calibration curve.

Chemical analysis and MALDI-TOF experiments were performed by the Laboratoire Central d'Analyses of the National French Research Council (CNRS) in Vernaison, France.

The contact angles of water have been measured with a DIGIDROP contact angle meter device (GBX Scientific

(27) Gottlieb, H. E.; Kotlyar, V.; Nudelman, A. *J. Org. Chem.* **1997**, *62*, 7512–7515.
(28) Roisnel, T.; Rodríguez-Carvajal, J. In *Materials Science Forum, Proceedings of the Seventh European Powder Diffraction Conference* (*EPDIC 7*); May 20/23, 2000; Delhez, R., Mittenmeijer, E. J., Eds.; Materials Science Forum: Barcelona, Spain, 2000; pp 118–123.
(29) Rodríguez-Carvajal, J.; Roisnel, T. Commission For Powder Diffraction, International Union for Crystallography **1998**, Newsletter 20 (May–August).

Scheme 2. Synthesis of 3a/3b by Acylation of 2a/2b with Methacryloylchloride

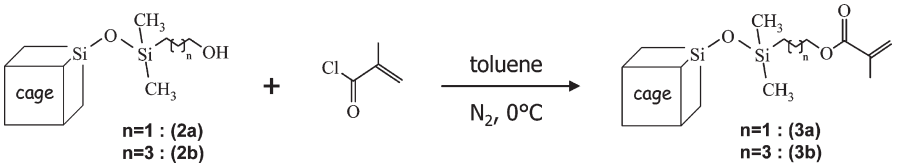

Instruments). A drop was deposited on the film surface with a microsyringe and then observed with a digital camera; its dimensions were calculated with the software Windrop. Each presented result corresponds to an average over 10 measurements. The wettability measurements were performed with distillated water and a dispersive liquid, diiodomethane, to determine the dispersive and polar components of the total surface energy.

XPS spectra were recorded using a PHOIBOS 100 X-ray photoelectron spectrometer from SPECS Company with the Mg Kα X-ray source ($h\nu$ = 1253.6 eV). The pass energy was set at 20 and 10 eV for the survey and the narrow regions (C 1s, O 1s, N 1s, Si 2p, and Na 1s), respectively.

The morphology of hybrid coatings was observed using scanning electron microscopy (SEM JEOL JSM-5500 at 10 up to 20 kV) with energy dispersive analyzer (EDX) to determine the composition of the nanocomposite coatings.

Results and Discussion

Part 1: DMIPOSS Derived Precursors and Characterizations. Addition of Si−H, catalyzed by platinum derivatives, on unsaturated alcohols can lead to two competitive reactions: hydrosilylation (or hydrosilation) and dehydrogenation (or dehydrocoupling) (Scheme 1).[23] Only hydrosilylation is of interest in this work.

ATR-FTIR spectra were recorded on the reacting mixtures before and after reaction. The spectra evolution (Table S1, Supporting Information) shows the disappearance of Si−H groups during the hydrosilylation of allylalcohol with DMIPOSS (ν_{Si-H} at 2142 cm^{-1} and δ_{Si-H} at 902 cm^{-1}); however, the reaction pathway could not be estimated from the evolution of the relative intensities of the stretching vibrations of C=C and OH (respectively $\nu_{C=C}$ at 1644 cm^{-1} and ν_{OH} at 3300 cm^{-1}) due to the fact that these signals were too weak to be detected and/or overlap with the signals of toluene.

To further characterize the allylalcohol and 4-penten-1-ol derivatives, ^{29}Si NMR experiments were performed (Table S2, Supporting Information). DMIPOSS showed T_3, Q_4, and M^H units (three peaks with 3:3:1 ratio for T_3, in agreement with trigonal distortion of DMIPOSS).[30] After reaction of DMIPOSS with both alcohols, a total conversion of M^H to M_1 sites was observed excluding dehydrogenation that would create D units. Only slight changes in the T_3 and Q_4 chemical shifts and intensities were observed, demonstrating the preservation of the inorganic cores.

Moreover, the hydrosilylation reaction can proceed by α- and β-addition leading to a mixture of products, even if the less hindered β-addition product is generally expected.[31] To check the regioselectivity of the reaction, ^{13}C NMR experiments were performed on hydroxyl-functionalized DMIPOSS **2a** and **2b**. The ^{13}C resonances were assigned with DEPT-135 experiments (Figure S1, Supporting Information). The absence of new peaks associated to CH or CH_3 groups as compared to DMIPOSS leads to the conclusion that only β-hydrosilylation occurred. Furthermore, the careful analysis of the data revealed the splitting of the peaks relative to $SiCH_2CH(CH_3)_2$ (three signals) and $SiCH_2CH(CH_3)_2$ (two signals) due to the trigonal distortion of the POSS cage. Similar ^{13}C NMR results were obtained for hydroxypropyl-DMIPOSS (**2a**).

Considering our results, it appears that clean and full hydrosilylation of allylalcohol and 4-penten-1-ol can also be performed with a monofunctional POSS. Zhang et al. considered the polyfunctionality of POSS as an important parameter in such type of reactions.[23]

Hydroxy-functionalized DMIPOSS **2a** and **2b** were reacted by acylation with methacryloylchloride (Scheme 2). The reaction products were obtained as white powders after precipitation in acetonitrile, dried under vacuum, and characterized to determine the extent of acylation.

The infrared spectra recorded on solid samples (Table S1, Supporting Information) indicate the presence of unpolymerized methacrylate groups at 1639 cm^{-1} ($\nu_{C=C}$) and 1724 cm^{-1} ($\nu_{C=O}$). No trace of methacryloyl chloride was detected (absence of ν_{C-Cl} at 874 cm^{-1} and the corresponding overtone at 1736 cm^{-1}). Low frequency bands (742 and 770−780 cm^{-1}) were systematically observed for **1**, **2a/b**, and **3a/b**. Such bands can be considered as characteristic for the Si_8O_{12} cubane structures.[32] ^{13}C NMR results, presented in a previous and preliminary work,[25] demonstrated the effective grafting of methacrylate groups. According to ^{1}H and ^{13}C NMR results, no extended polymerization occurs during functionalization. Nevertheless, the formation of dimers or small oligomers cannot be excluded. Sellinger et al. reported that such an issue could be addressed by SEC.[33] In the following, all molecular weights measured by SEC are given in PS equivalents, and there is no reason for an exact match with the real molecular weight. Indeed, SEC is based on differences in hydrodynamic volumes. Because of the relationship between hydrodynamic volume and molecular weight depending on the species, only approximate measurements can be achieved when the nature of

(30) Bonhomme, C.; Toledano, P.; Maquet, J.; Livage, J.; Bonhomme-Coury, L. *J. Chem. Soc., Dalton Trans.* **1997**, 1617–1626.
(31) Kendrick, T. C.; Parboo, B.; White, J. W. In *The Chemistry of organic silicon compounds*; Patai, S., Rappoport, Z., Eds.; Wiley: New-York, 1989; Vol. *2*, Chap. 21.
(32) Calzaferri, G.; Imhof, R.; Törnroos, K. W. *J. Chem. Soc., Dalton Trans.* **1994**, 3123–3128.
(33) Sellinger, A.; Laine, R. M. *Macromolecules* **1996**, *29*, 2327–2330.

Table 1. MALDI-TOF MS Data (Da) for 1, 3a, and 3b (cationization agent: NaI, Matrix: 2,5-dihydroxybenzoic acid)

sample	obs. mass	assignment (calc. mass)
1	889.5	$[\mathbf{1}]^+$ (890.3)
	913.4	$[\mathbf{1}+Na]^+$ (913.3)
	999.5	$[\mathbf{XSiH}]^{+a}$
3a	889.4	$[\mathbf{1}]^+$ (890.3)
	971.5	$[\mathbf{2a}+Na]^+$ (971.3)
	1039.5	$[\mathbf{3a}+Na]^+$ (1039.3)
	1075.5	$[\mathbf{Y}]^{+\,a}$
	1125.6	$[\mathbf{XSi}(CH_2)_3OC(O)C(CH_3)CH_2]^+$ (*998.5* + 127.1)
	1279.7	$[\mathbf{XSi}(CH_2)_3OC(O)C(CH_3)CH_2+$ Matrix$]^+$ (*998.5* + 127.1 + 154.0)
	2074.9	$[\mathbf{2a}+\mathbf{XSi}(CH_2)_3OC(O)C(CH_3)CH_2]^+$ (948.3 + *998.5* + 127.1)
3b	889.5	$[\mathbf{1}]^+$ (890.3)
	999.5	$[\mathbf{2b}+Na]^+$ (999.3)
	1067.5	$[\mathbf{3b}+Na]^+$ (1067.4)
	1103.5	$[\mathbf{Y}(CH_2)_2]^+$ (*1075.5* + 28.0)
	1153.6	$[\mathbf{XSi}(CH_2)_5OC(O)C(CH_3)CH_2]^+$ (*998.5* + 155.1)
	1307.7	$[\mathbf{XSi}(CH_2)_5OC(O)C(CH_3)CH_2+$ Matrix$]^+$ (*998.5* + 155.1 + 154.0)
	2129.9	$[\mathbf{2b}+\mathbf{XSi}(CH_2)_5OC(O)C(CH_3)CH_2]^+$ (976.3 + *998.5* + 155.1)

[a] The mass observed for the unknown species XSiH and Y might include a sodium ion. If so, the calculations assume that their derivatives include also a sodium ion.

the calibration standards is different from the studied sample.

The size exclusion chromatogram of **1** was bimodal with one main peak at M_n = 760 g·mol^{-1} with a polydispersity index (PDI) of 1.00, and a minor peak, centered at M_n = 2040 g·mol^{-1} with a PDI of 1.20, likely due to some impurities (the nature of the corresponding impurities will be emphasized by MALDI-TOF experiments vide infra). The chromatograms of both new functionalized NBBs (**3a** and **3b**) were also bimodal. The first sharp and intense peak is centered on 860 (**3a**) and 880 g·mol^{-1} (**3b**) with PDI of 1.01 for both compounds. The second peak, broader and less intense, is centered on 1930 (**3a**, PDI = 1.08) or 2210 g·mol^{-1} (**3b**, PDI = 1.16). These second peaks could correspond to dimers.

To clarify this point MALDI-TOF mass spectrometry experiments were performed on **1**, **3a**, and **3b** (cationization agent: NaI, absorbing matrix: 2,5-dihydroxybenzoic acid). MALDI has been successfully applied for the characterization of hexasilsesquioxanes units.[34] MALDI-TOF experiments have been performed also for the fine description of propyl-methacrylate POSS oligomers[35] and POSS siloxane dimers and trimers,[36] as well as POSS containing encapsulated fluoride ions.[37]

Results are presented in Table 1 (as well as in Figures S2 and S3, Supporting Information). For **1**, the main peaks correspond to $[DMIPOSS]^+$ and $[DMIPOSS+Na]^+$. There is also a minor peak at 999.5, for which no formula could be suggested but which corresponds to a compound bearing a Si−H group as it is affected by hydrosilylation (vide infra); in the following this unknown species will be labeled XSiH. Several very minor peaks are present in the range 1700−1900 and might explain the minor peak in the SEC experiment.

The major peak in the mass spectrum of **3a** corresponds to the expected methacrylate functionalized POSS. Almost all the other peaks can be reasonably well explained. First, small amounts of **1** and **2a** are observed. Then, the peak at 1075.5 is not identified but likely comes from a species (labeled Y in Table 1) that has reacted with allyl alcohol. Indeed, in the mass spectrum of **3b** a similar species is found with 28 additional mass units, as expected when allylalcohol is substituted for 4-penten-1-ol. The peak at 1125.6 clearly results from the two step functionalization (hydrosilylation and acylation) of the unknown impurity XSiH (in **1**) by a 3-propylmethacrylate group. The peak at 1279.7 is associated with an adduct between the functionalized XSiH and a matrix molecule (M_w = 154.0 g·mol^{-1}). Finally, the peak at 2074.9 does not correspond to a dimer "**3a**+**3a**" but to the association of **2a** with functionalized XSiH.

The present interpretation of the mass spectrum of sample **3a** can be exactly transposed to sample **3b**, just taking into account the extra 28 mass units introduced by replacing of the propyl spacer with a pentyl group.

In conclusion, MALDI-TOF MS shows that no dimer "**3a**+**3a**" (or "**3b**+**3b**") is formed during functionalization. Moreover, it indicates that the high mass species observed by SEC is derived from an unknown impurity in **1**. The various minor species present in samples **3a** and **3b** likely explain the small discrepancies observed in the elemental analyses (see Supporting Information). However, because of the non-quantitative nature of the MALDI-TOF and the absence of spurious signals in NMR (^{1}H, ^{13}C, and ^{29}Si), samples **3a** and **3b** were considered as pure.

DSC provides clearly defined melting points (T_m) of 264, 143, 137, 126, and 116 °C for compounds **1**, **2a**, **2b**, **3a**, and **3b**, respectively. Crystallization could also be observed for each compound during the cooling step. Both features are a strong indication of the purity of the samples. T_m decreases as the length of the pending group increases, as shown by Bölln et al.[38] (who mentioned the role of the alkyl chain length in the thermal behavior of the homologous series of octa-*n*-alkylsubstituted T_8 derivatives). The thermal properties of PEG octafunctionalized POSS (with variable PEG chains) and PEO/POSS derivatives were also extensively studied by Markovic et al.[24] and Maitra et al.,[39] respectively.

Discussion on Powder XRD. The powder XRD of **1**, **2a**, **2b**, **3a**, and **3b** were analyzed, between 6° and 50° (2θ). Experimental and calculated XRD patterns are presented

(34) Bassindale, A. R.; MacKinnon, I. A.; Maesano, M. G.; Taylor, P. G. *Chem. Commun.* **2003**, 1382–1383.
(35) Anderson, S. E.; Baker, E. S.; Mitchell, C.; Haddad, T. S.; Bowers, M. T. *Chem. Mater.* **2005**, *17*, 2537–2545.
(36) Anderson, S. E.; Mitchell, C.; Haddad, T. S.; Vij, A.; Schwab, J. J.; Bowers, M. T. *Chem. Mater.* **2006**, *18*, 1490–1497.
(37) Anderson, S. E.; Bodzin, D. J.; Haddad, T. S.; Boatz, J. A.; Mabry, J. M.; Mitchell, C.; Bowers, M. T. *Chem. Mater.* **2008**, *20*, 4299–4309.
(38) Bölln, C.; Tsuchida, A.; Frey, H; Müllhaupt, R. *Chem. Mater.* **1997**, *9*, 1475–1479.
(39) Maitra, P.; Wunder, S. L. *Chem. Mater.* **2002**, *14*, 4494–4497.

Table 2. XRD Data for Compounds 1, 2a, 2b, 3a, and 3b

compound	a_{hex} (Å)	c_{hex} (Å)	c_{hex}/a_{hex}	a_{rh} (Å)	α_{rh} (deg)
1	16.110	17.135	1.064	10.915	95.120
2a	16.207	17.171	1.059	10.969	95.254
2b	16.040	17.010	1.060	10.859	95.222
3a	16.219	17.204	1.061	10.980	95.214
3b	16.117	17.110	1.062	10.914	95.185

in Figures S4−S7 (Supporting Information). They can be indexed with hexagonal unit cells as are many other POSS related compounds.[30,40−55] Results are reported in Table 2. As noted by Fu et al.,[54] corner substitution has little effect on the crystal structure. Yet, the diffraction lines are broader than those observed for a symmetrical POSS (e.g., octacyclohexyl-POSS).[54] This feature could arise from smaller crystals or defects associated with packing of the POSS pendant group. A closer look at the Miller indices ($-h + k + l = 3n$) shows that the chosen hexagonal cell is a multiple one, the primitive unit cell being rhombohedral ($a_{rh} = b_{rh} = c_{rh}$ and $\alpha_{rh} = \beta_{rh} = \gamma_{rh}$).

For the five compounds, the c_{hex}/a_{hex} ratio equals 1.06. These values compare very well with those reported by Waddon et al.,[40] who discussed these c_{hex}/a_{hex} ratios in relation to the much larger theoretical value, $\sqrt{6}$ (∼2.45), observed for a close packing of hard spheres (in a fcc network: ABCA stacking sequence). To explain this large discrepancy, they suggest that the groups linked to the corners of the POSS are responsible for the absence of close packing in the basal planes (larger a_{hex}), which enables adjacent layers to approach more closely (smaller c_{hex}).

Actually, the c_{hex}/a_{hex} ratios reported in the present work, as well as those reported by Waddon et al.[40] and those of a great deal of POSS related compounds (Table S3, Supporting Information), compare much better to $\sqrt{3}/\sqrt{2}$ (∼1.22), which is the theoretical ratio for the hexagonal description of a simple cubic packing (Figure 1). Indeed, for such a packing an ABCA stacking sequence is also observed along the [111] direction (Figure 1). Even the ratio c_{hex}/a_{hex} for $H_8Si_8O_{12}$ (which equals 1.67) is still closer to 1.22 than to 2.45. Moreover, for a fcc packing, the primitive unit cell is rhombohedral with an angle of 60°, while the primitive cell for many POSS, including compounds **1**, **2a**, **2b**, **3a**, and **3b**, is rhombohedral but with an angle ∼95° (Table 2 and Table S3, Supporting Information).

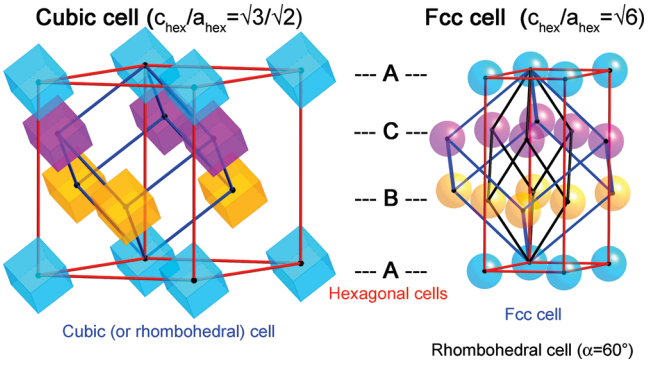

Figure 1. Comparison between cubic packing and face centered cubic (fcc) packing, highlighting the change in the c_{hex}/a_{hex} ratio for the corresponding hexagonal cells.

In conclusion, POSS are usually considered to exhibit spherical shapes and are therefore expected to pack accordingly on a fcc network, but according to the observed c_{hex}/a_{hex} ratios and rhombohedral angles, they appear to behave more like cubes that pack on a simple cubic network, yet with a slight distortion, to achieve the best possible packing of the various groups attached to their corners. Such a preference of cubic shaped objects for simple cubic packing has also been observed on a totally different scale in colloidal crystal.[56]

Part 2: Film Preparation, Characterizations, and Hydrophobic Properties. The monofunctional POSS was reacted with cyclohexylmethacrylate (CHMA) and tetra-ethoxylated bisphenol A dimethacrylate (Bis-EMA) at various weight percents. ^{i}BuPOSSMA, **3a**, and **3b** were miscible in the CHMA/Bis-EMA matrix at concentrations of 1−2 wt % (see SEM in the backscattered electron mode in Figure 2a,b). After UV curing, the coatings were transparent and provided free-standing films. At concentrations of 5 and 10 wt %, ^{i}BuPOSSMA was found to be miscible in the MA matrix whereas **3a** and **3b** were barely miscible, leading to yellowish and translucent films after peeling. SEM observations confirmed that a phase separation occurs at the film surface during polymerization for 10 wt % of **3a** (similar results were obtained for **3b** based films): small dispersed aggregates were observed (Figure 2c). EDX analyses indicated higher silicon contents (between 12 and 19 atom %) in the small aggregates (zones 2 and 3 of the micrograph) than in darker regions (7 atom % of Si atoms in zones 1 and 4), suggesting that they are mainly constituted of POSS. XRD patterns of

(40) Waddon, A. J.; Coughlin, E. B. *Chem. Mater.* **2003**, *15*, 4555–4561.
(41) Provatas, A.; Luft, M.; Mu, J. C.; White, A. H.; Matisons, J. G.; Skelton, B. K. *J. Organomet. Chem.* **1998**, *565*, 159–164.
(42) Larsson, K. *Ark. Kemi* **1960**, *16*, 215–219.
(43) Barry, A. J.; Daudt, W. H.; Domicone, J. J.; Gilkey, J. W. *J. Am. Chem. Soc.* **1955**, *77*, 4248–4252.
(44) Larsson, K. *Ark. Kemi* **1960**, *16*, 209–214.
(45) Koellner, G.; Mueller, U. *Acta Crystallogr., Sect. C* **1989**, *C45*, 1106–1107.
(46) Toernroos, K. W. *Acta Crystallogr., C* **1994**, *C50*, 1646–1648.
(47) Toernroos, K. W.; Calzaferri, G.; Imhof, R. *Acta Crystallogr., C* **1995**, *C51*, 1732–1735.
(48) Rebrov, E. A.; Tebeneva, N. A.; Muzafarov, A. M.; Ovchinnikov, Y. E.; Struchkov, Y. T.; Strelkova, T. V. *Russ. Chem. Bull.* **1995**, *44*, 1286–1292.
(49) Unno, M.; Takada, K.; Matsumoto, H. *Chem. Lett.* **1998**, *6*, 489–490.
(50) Unno, M.; Suto, A.; Takada, K.; Matsumoto, H. *Bull. Chem. Soc. Jpn.* **2000**, *73*, 215–220.
(51) Said, M. A.; Roesky, H. W.; Rennekamp, C.; Andruh, M.; Schmidt, H.-G.; Noltemeyer, M. *Angew. Chem., Int. Ed.* **1999**, *38*, 661–664.
(52) Feher, F. J. W., K.D.; Baldwin, R. K.; Soulivong, D.; Lichtenhan, J. D.; Ziller, J. W. *Chem. Commun.* **1999**, 1289–1290.
(53) Auner, N.; Ziemer, B.; Herrschaft, B.; Ziche, W.; John, P.; Weis, J. *Eur. J. Inorg. Chem.* **1999**, 1087–1094.
(54) Fu, B. X.; Hsiao, B. S.; Pagola, S.; Stephens, P.; White, H.; Rafailovich, M.; Sokolov, J.; Mather, P. T.; Jeon, H. G.; Phillips, S.; Lichtenhan, J.; Schwab, J. *Polymer* **2001**, *42*, 599–611.
(55) Bassindale, A. R.; Chen, H.; Liu, Z.; MacKinnon, I. A.; Parker, D. J.; Taylor, P. G.; Yang, Y.; Light, M. E.; Horton, P. N.; Hursthouse, M. B. *J. Organomet. Chem.* **2004**, *689*, 3287–3390.
(56) Li, F.; Delo, S. A.; Stein, A. *Angew. Chem., Int. Ed.* **2007**, *46*, 6666–6669.

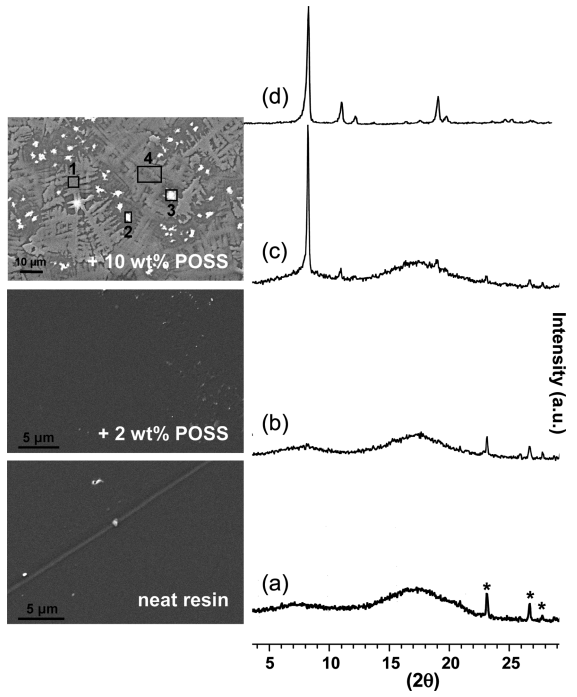

Figure 2. XRD patterns and SEM micrographs of (a) MA neat resin, (b) 2 wt % of **3a** in MA resin, (c) 10 wt % of **3a** in MA resin, and (d) compound **3a**. *: substrate.

hybrid films were in good agreement with SEM-EDX observations. Indeed, POSS crystallization was observed at 10 wt % POSS concentration, whereas the XRD patterns of films with 1 and 2 wt % POSS were similar to the patterns of the neat resin (Figure 2a−d).

To characterize more thoroughly the surface properties of the hybrid films, contact angle experiments were performed with water on both sides of the free-standing films (Table 3). Similar contact angle values (73−80°) were found for the sides exposed to the glass substrates during the UV-curing. But interestingly, major changes depending on the POSS filler were observed for the air sides. The contact angle θ for the neat resin is 67°. The introduction of 2 wt % of ^{i}BuPOSSMA increases θ by ~20° whereas 2 wt % of either **3a** or **3b** increases θ by ~30°. It is worth mentioning that the incorporation of polydimethylsiloxane (PDMS) in polymers at small % loadings can lead also to increased hydrophobic properties.

This increase suggests enrichment of the air-coating interface by POSS, as recently shown for other POSS modified polymer systems.[19,57,58] For **3a** and **3b**, a strong effect was observed for lower POSS loadings with respect to these previous studies (1 wt % vs ca. 2 wt % of a fluorinated POSS[19,57] or 3 wt % of isobutylPOSS[58]). This feature can likely be related to the process in which a coating of highly mobile monomers is first formed and then polymerized by UV, while in these other studies coatings are cast from solutions of POSS-modified polymers.[19,57,58] In our results, the contact angle is higher for **3a** and **3b** than for ^{i}BuPOSSMA for both 1 and 2 wt % compositions. This may arise from the more flexible Si−O−Si link between the methacrylate group and POSS core, which could make more efficient the positioning of the bulky hydrophobic $^{i}Bu_7Si_8O_{12}$ cage at the air−film interface.

Table 3 also reports the values of the polar (γ_S^p) and dispersive (γ_S^d) components of the surface energy (γ_S), calculated according the Owens-Wendt theory.[59] The incorporation of small amounts of POSS decreases the total surface energy from 50 to 35 mJ·m^{-2}; the polar component seems to be particularly sensitive to the presence of even 1 wt % of POSS in the methacrylate matrix, as recently reported by Turri et al.[58]

XPS spectra of neat resin and films made from ^{i}BuPOSSMA and **3a** (2 wt % in resin) were recorded on both air and glass sides of the films. Table 4 shows the atomic percentages of the main elements present in the near-surface region of the film (air-side and glass-side).

One can notice that the glass side of all coatings is systematically contaminated by sodium which originates from the glass formulation. Carbon and oxygen are present in relative proportions corresponding to the composition of the methacrylic resin. The N 1s peak is due to N-methyl diethanol amine contained in the photocuring set (see the Experimental Section). The introduction of 2 wt % of ^{i}BuPOSSMA led to an increase of the silicon and oxygen contents and a decrease of the carbon content, indicating the presence of POSS at the surface of the films. Nevertheless, the N 1s peak remained, suggesting that POSS are not covering the whole surface of the film. The introduction of 2 wt % of **3a** led to a stronger increase of the silicon content, demonstrating higher POSS concentration at the surface of the film. Nitrogen was not observed on the XPS spectrum, suggesting that in that case POSS are covering the whole surface of the film.

High resolution O 1s spectra were performed for the six samples (both faces of the three films). A broad peak was observed in both spectra of the MA resin coating (air- and glass-side). This peak became sharper on the air-side spectra, by introducing 2 wt % of POSS (either ^{i}BuPOSSMA or **3a**) whereas it remained broad on the glass-side spectra. This is in good agreement with the suggestion that POSS could cover the surface of the polymer film.

For all samples, the C 1s peak was fitted with three components (Figure S8, Supporting Information) centered at ~285.0, ~286.6, and ~288.8 eV corresponding to C—C/C—H, C—O, and C═O (ethoxy and ester functional groups). The first peak which corresponds to polymer and C contamination was used as an internal reference. The C═O component (characteristic of methacrylic resin) is strongly attenuated by increasing the silicon content. This attenuation allowed us to estimate the POSS layer thickness (d), calculated from the relative intensities of the C 1s signals and using the Beer−Lambert equation applied for C 1s:

$$I_{C1s} = I_{Cls}^{\infty} \exp\left[\frac{-d}{\lambda_{C1s}}\right] \quad (1)$$

(57) Iacono, S. T.; Budy, S. M.; Mabry, J. M.; Smith, D. W., Jr. *Macromolecules* **2007**, *40*, 9517–9522.
(58) Turri, S.; Levi, M. *Macromol. Rapid Commun.* **2005**, *26*, 1233–1236.
(59) Owens, D. K.; Wendt, R. C. *J. Appl. Sci.* **1969**, *13*, 1741–1747.

Table 3. Contact Angle (θ) Measurements and Polar and Dispersive Components of the Surface Energy

film composition	$\theta \pm$ SD (deg) "glass side"	$\theta \pm$ SD (deg) "air side"	γ_S^d (mJ·m^{-2})	γ_S^p (mJ·m^{-2})	γ_S (mJ·m^{-2})
neat resin (CHMA/Bis-EMA)	73 ± 4	67 ± 5	42 ± 2	8 ± 2	50 ± 3
[i]BuPOSSMA (1 wt %) in resin	76 ± 2	87 ± 4	38 ± 1	2 ± 1	40 ± 2
3a (1 wt %) in resin	76 ± 2	95 ± 1	33 ± 1	0 ± 1	35 ± 2
3b (1 wt %) in resin	79 ± 4	97 ± 4	35 ± 1	0 ± 1	35 ± 2
[i]BuPOSSMA (2 wt %) in resin	77 ± 1	75 ± 6			
3a (2 wt %) in resin	77 ± 2	100 ± 2			
3b (2 wt %)in resin	80 ± 2	102 ± 3			

Table 4. Summary of XPS Elemental Concentrations and Binding Energies of POSS Based Films

	elemental atomic percent					binding energy, eV (relative % area) C 1s		
film composition	C 1s	O 1s	Si 2p	Na 1s	N 1s	C—C/C—H	C—O	C=O
neat resin (CHMA/Bis-EMA) (*air-Side*)	72.8	24.1	2.2		0.9	285.0 (67%)	286.6 (27%)	288.9 (6%)
neat resin (CHMA/Bis-EMA) (*glass-Side*)	78.4	18.7	1.0	1.8		284.9 (72%)	286.5 (21%)	288.8 (7%)
[i]BuPOSSMA (2 wt %) in resin (*air-Side*)	68.7	26.1	4.3		0.9	285.0 (68%)	286.6 (25%)	288.9 (7%)
[i]BuPOSSMA (2 wt %) in resin (*glass-Side*)	76.5	19.3	0.4	3.8		284.9 (73%)	286.5 (21%)	288.8 (6%)
3a (2 wt %) in resin (*air-Side*)	60.6	27.3	12.0			285.0 (81%)	286.5 (15%)	288.7 (4%)
3a (2 wt %) in resin (*glass-Side*)	76.6	19.8	0.4	3.3		285.0 (74%)	286.5 (20%)	288.9 (6%)

where I_{C1s} is the intensity of the C 1s signal from the film made from POSS and I^{∞}_{C1s} is the C 1s peak intensity for an infinitely thick MA resin film. λ_{C1s} is the C 1s electron mean free path in the POSS layer. λ_{C1s} can be calculated using the equation of Seah and Dench:[60]

$$\lambda = 0.11 \cdot E_k^{1/2} + 49 \cdot E_k^{-2} \qquad \text{(Eq.2)}$$

where $E_k = h\nu - E_b$. E_k is the kinetic energy (eV) of a particular electron crossing the overlayer; $h\nu$ is the X-ray energy (1253.6 eV), and E_b is the C 1s binding energy (about 285 eV). Therefore $E_k = 968.6$ eV and $\lambda \sim 3$ nm, assuming that $\rho = 1.158$ g·cm^{-3} for [i]BuPOSS MA and **3a**.[61] Thus, the thickness (d) was estimated at 1.7 ± 0.2 nm. Considering that the octafunctional POSS are 1.2−1.4 nm in diameter,[14] the estimated thickness suggests that POSS **3a** can pack as a monolayer at the film surface.

The *dissymmetry* found in our films is an interesting point. In a previous work,[19] neutron reflectivity showed a *symmetric* enrichment of both faces of coatings deposited on silicon wafers (always covered by a thin layer of native silica) from solutions of preformed POSS-terminated polymers. The dissymmetry observed for our films may arise from their preparation. Indeed, POSS-based monomers can likely move more easily and on larger distances than bulky POSS-based polymers and, therefore, enable a higher enrichment of the more hydrophobic air−liquid interface than of the more hydrophilic glass−liquid interface. Such effects were indeed observed for free POSS, $(C_5H_9Si)_7SiRO_{12}$ (R: $(CH_2)_2-(CF_2)_7CF_3$ or $CH_2CH(OH)CH_2OH$), mixed in a polystyrene coating on silicon wafer. When the POSS bears a $(CH_2)_2-(CF_2)_7CF_3$ group (hydrophobic), the air−film interface is enriched in POSS, while when it had a $CH_2CH(OH)CH_2OH$ group (hydrophilic), the silica−film interface is enriched.[20] Thermal gradients introduced by the UV irradiation in the coatings depth may also play some role in the dissymmetry.

Conclusions

In this article, we demonstrate facile monofunctionalization of POSS obtained by hydrosilylation of allylalcohol and 4-penten-1-ol. Polyfunctionality of the POSS entities does not seem necessary. The observed c_{hex}/a_{hex} ratios show that the crystalline packing of the POSS described in this work, as well as the one of many others, is closer to the simple cubic network than to the face centered cubic network usually considered for spheroidal objects.

In a second part, we showed that the surface properties of the hybrid coatings made from CHMA/Bis-EMA and alkylmethacryloxy-DMIPOSS were strongly modified even for very low content of POSS (1 or 2 wt %). The incorporation of small amounts of POSS strongly enhanced the contact angle (an increase of almost 30° was observed) whereas the total surface energy of the coated surface was reduced. XPS spectra have revealed high silicon content at the surface of the films, leading to the conclusion that POSS are well packed at the surface of the coatings.

Acknowledgment. The authors gratefully thank Riccardo Ceccato (XRD experiments), Marco Amici and Jocelyne Galy (SEC experiments), Jean-François Gérard (surface

(60) Seah, M. P.; Dench, W. A. *Surf. Interface Anal.* **1979**, *1*, 2–7.
(61) Bizet S. Ph.D. of Institut National de Sciences Appliquées (INSA), Lyon, France, 2004.

properties), Christophe Méthivier (XPS measurements), and Celine Fosse (discussion on MS). Marie-Noëlle Rager is also kindly acknowledged for fruitful discussions during NMR experiments. F.M. acknowledges the financial support provided through the European Community's Human Potential Program under the contract HPRN-CT-2002-00306 [NBB-Hybrids].

Supporting Information Available: ^{13}C DEPT-135 NMR for **2b**, MALDI-TOF MS for **1**, **3a**, and **3b**, experimental and simulated XRD patterns for **1**, **2a**, **2b**, **3a**, and **3b**, high resolution XPS spectra for films, and IR and ^{29}Si NMR data for **1**, **2a**, **2b**, **3a**, and **3b**, as well as cell parameters for various POSS related compounds (PDF). This material is available free of charge via the Internet at http://pubs.acs.org.